First-Order Vortex Lattice Melting and Magnetization of $YBa_2Cu_3O_{7-\delta}$

R. Šášik and D. Stroud
Department of Physics, The Ohio State University, Columbus, Ohio 43210
(Received 15 June 1995)

We present the first non-mean-field calculation of the magnetization $M(T)$ of $YBa_2Cu_3O_{7-\delta}$ both above and below the flux-lattice melting temperature $T_m(H)$, in good agreement with experiment. Fluctuations in both order parameter $\psi(\mathbf{r})$ and magnetic induction B are included in the Ginzburg-Landau free energy. The second derivative $(\partial^2 M/\partial T^2)_H$ is predicted to be negative throughout the vortex liquid state and positive in the solid state. The discontinuity in entropy at melting is calculated to be $\sim 0.034 k_B$ per flux line per layer at 50 kOe.

PACS numbers: 74.60.–w, 74.25.Dw, 74.25.Ha, 74.40.+k

Even more than perfect conductivity, the magnetization $\mathbf{M}$ is a sensitive probe of the superconducting state. In this paper we calculate the magnetization of the most studied high-T_c material, $YBa_2Cu_3O_{7-\delta}$, including the effects of fluctuations [1,2]. We consider an applied field $\mathbf{H}\|c$, and also calculate the first-order flux-lattice melting curve $T_m(H)$ for the same material. Both $\mathbf{M}$ and $T_m(H)$ are in very good agreement with experiment over a range of magnetic fields.

Our approach is to start from a Ginzburg-Landau free energy functional that includes the field energy in the form [3]

$$G[\psi,\mathbf{A}] = \int d^3\mathbf{r}\left\{a(T,z)|\psi(\mathbf{r})|^2 + \frac{1}{2m^*}\left|\left(-i\hbar\nabla - \frac{e^*}{c}\mathbf{A}(\mathbf{r})\right)\psi(\mathbf{r})\right|^2 + \frac{b}{2}|\psi(\mathbf{r})|^4 + \frac{(\mathbf{B}-\mathbf{H})^2}{8\pi}\right\}. \quad (1)$$

Here $\psi(\mathbf{r})$ is the complex order parameter, $\mathbf{A}(\mathbf{r})$ is the vector potential, $\mathbf{B} = \nabla \times \mathbf{A}$, $e^* = 2e$ is the charge of a Cooper pair, $\mathbf{H} \equiv H\hat{\mathbf{z}}$ is the applied magnetic field intensity, and $a(T,z)$, b, and m^* are phenomenological parameters. The periodic z dependence of $a(T,z)$ is introduced to characterize the underlying layered structure. We assume that spatial modulation of $a(T,z)$, which acts as a potential for Cooper pairs, results in a tight-binding form for $\psi(\mathbf{r})$ along the z axis, thus creating the effective mass anisotropy γ. The integral is to be carried out over a fixed sample volume $V = (\phi_0/H)N_\phi N_z s$, where s is the periodicity of the layered structure, $\phi_0 = hc/2e$ is the flux quantum, N_ϕ is the number of flux lines threading the sample, and N_z is the number of layers. The Gibbs free energy density appropriate to an experiment at fixed T and $\mathbf{H}$ is

$$\mathcal{G} = -(k_B T/V)\ln Tr_{\psi,\mathbf{A}} \exp(-G[\psi,\mathbf{A}]/k_B T). \quad (2)$$

We also define free energy "per flux line per layer" according to $\mathcal{G}_\phi \equiv (\phi_0 s/H)\mathcal{G}$; the internal energy G_ϕ and entropy S_ϕ are defined in the same fashion.

To determine the magnetization, we assume a *uniformly fluctuating* magnetic induction $\nabla \times \mathbf{A}(\mathbf{r}) \equiv B\hat{\mathbf{z}}$, so that B can in principle assume different values in the flux liquid and solid phases. This approximation is most reasonable in the extreme type-II limit ($\kappa \gg 1$) when density correlations among the vortices are well developed and vortices are clearly defined, as expected in the neighborhood of the melting line. In addition, the assumption of uniform $\mathbf{B}$ should be best in the vortex liquid phase, where contributions to the local field $\mathbf{B}(\mathbf{r})$ come from many positionally uncorrelated vortex line segments, as suggested by Brandt [4], but may still be reasonable in the vortex solid phase, even though $\mathbf{B}$ in that phase should develop a nonzero variance $\sigma^2 = \langle \mathbf{B}(\mathbf{r})^2\rangle - \langle \mathbf{B}(\mathbf{r})\rangle^2$.

We evaluate the statistical average (2) using the following procedure. First, we expand the order parameter $\psi(\mathbf{r})$ in a basis that consists of products of lowest Landau level states of the operator $(2m^*)^{-1}(-i\hbar\nabla_\perp - e^*\mathbf{A}/c)^2$ in the a-b plane, and Wannier functions from the lowest band of states of the operator $a(T,z) - (2m^*)^{-1}\hbar^2\partial^2/\partial z^2$ in the c direction [5]. This leads to an explicit form for all but the last term of the integrand in Eq. (1), in terms of the complex coefficients $c_{k,n}$ of the expansion, corresponding to the kth lowest Landau state in the nth layer [5]. Then the statistical average implied by Eq. (2) is carried out by a Monte Carlo (MC) procedure, in which the coefficients $c_{k,n}$, *and also the average magnetic induction* B, are considered as fluctuating MC variables. The entire procedure is closely analogous to the "constant pressure" MC ensemble well known in classical fluids [6]. The variables analogous to pressure and volume are H and B. The MC step that changes B increases or decreases the area of the a-b plane at constant vortex number.

Within this approach, the *mean-field approximation* to (2) is specified by a pair $\psi(\mathbf{r})$ and B, for which G is minimum [3]. In the normal state [$H > H_{c2}(T)$] this is achieved for $\psi(\mathbf{r}) = 0$ and $B = H$. In the mixed state, $H < H_{c2}(T)$, the corresponding minimum is attained for a triangular lattice of straight vortex lines and magnetization

$$M \equiv (B - H)/4\pi = [H - H_{c2}(T)]/4\pi(2\kappa^2\beta_A - 1), \quad (3)$$

 0031-9007/95/75(13)/2582(4)$06.00

where $\beta_A = 1.159\,59\ldots$ is the Abrikosov ratio. In the limit $\kappa \gg 1$ studied here, this formula becomes identical to the original Abrikosov result, which has $4\pi(2\kappa^2 - 1)\beta_A$ in the denominator. Thus our approach and approximations are indeed correct at the mean-field level in this limit. The corresponding mean-field free energy density is $\mathcal{G}^{\mathrm{MF}} = -(8\pi)^{-1}[H_{c2}(T) - H]^2/(2\kappa^2\beta_A - 1)$.

In order to execute the MC calculation for $YBa_2Cu_3O_{7-\delta}$, we use the following set of parameters: $T_{c0} = 93$ K, $dH_{c2}(T)/dT = -1.8 \times 10^4$ Oe/K, $s = 11.4$ Å, $\gamma = 5$, and $\kappa = 52$. Although there is some experimental evidence that κ varies with magnetic field [7], we neglect this field dependence here. In most of our calculations, we have considered a cell containing $N_\phi = 10^2$ vortices and $N_z = 10$ layers. Our results are based typically on $(2-3) \times 10^5$ MC passes through the entire sample following $\sim 2 \times 10^4$ MC passes for equilibration.

Figure 1 shows the calculated magnetization $M(T)$ of $YBa_2Cu_3O_{7-\delta}$ as a function of temperature T at three different values of H. The mean-field predictions are shown for comparison. There is no sign of a true phase transition at the mean-field transition temperature $T_{c2}(H)$,

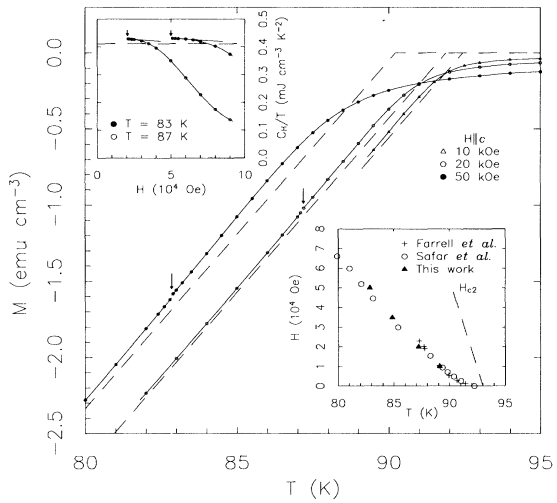

FIG. 1. Calculated magnetization $M(T)$ of $YBa_2Cu_3O_{7-\delta}$ at $H = 10$, 20, and 50 kOe. Dashed lines represent the mean-field solution (3). Solid lines are spline curves connecting the calculated points. Arrows denote melting temperatures $T_m(H)$, as determined by the discontinuity in $M(T)$. Estimated errors in $M(T)$ are much smaller than the symbol sizes. $N_\phi \times N_z = 10^2 \times 10$. Right inset: locus of the liquid-solid phase boundary in the H-T plane, as determined by our calculations and as measured by Farrell, Rice, and Ginsberg [8] and Safar *et al.* [9]. Left inset: specific heat C_H as a function of magnetic field, taken at two temperatures, $T = 83$ and 87 K. The dashed line represents the mean-field value C_H^{MF}/T. Arrows indicate the approximate location of the fields at melting $H_m(T)$. Straight lines have slopes -0.0038 emu cm^{-3} K^{-2} at 87 K and -0.0030 emu cm^{-3} K^{-2} at 83 K (see text). $N_\phi \times N_z = 6^2 \times 6$.

since $(\partial M/\partial T)_H$ is continuous at that point. Instead, there is an apparently first-order melting transition at a lower temperature $T_m(H)$, as signaled by a weak discontinuity in the magnetization curves (denoted by arrows in the figure). The melting curve $T_m(H)$ inferred from this discontinuity is shown in the inset to Fig. 1; it is in good agreement with experiment.

The general behavior of $M(H,T)$ agrees very well with experiment [10]. For example, the calculated second derivative $(\partial^2 M/\partial T^2)_H$ is negative throughout the vortex liquid phase, in accord with recent measurements based on a differential torque technique [11]. A second-degree polynomial fit to our magnetization results just above the melting temperature T_m yields $(\partial^2 M/\partial T^2)_H = -0.0038 \pm 0.002$ emu cm^{-3} K^{-2} for $H = 20$ kOe, and $(\partial^2 M/\partial T^2)_H = -0.0030 \pm 0.002$ emu cm^{-3} K^{-2} for $H = 50$ kOe. Experiment [11] also gives a negative $(\partial^2 M/\partial T^2)_H$ for fields in the range 10–20 kOe, and of the same order of magnitude. In the solid phase, we find our calculated $(\partial^2 M/\partial T^2)_H > 0$.

Another striking feature of our results is the crossing of the magnetization curves as a function of temperature. This crossing is also observed in experiment at a similar temperature [10]. In $Bi_2Sr_2CaCu_2O_{8+\delta}$, the same phenomenon has attracted much theoretical attention [12,13], because it is believed to occur at a unique temperature T^* independent of field. In $YBa_2Cu_3O_{7-\delta}$, experimental data of Welp *et al.* [10] reveal that magnetization curves do not cross at a single point, presumably because, although layered, $YBa_2Cu_3O_{7-\delta}$ is only moderately anisotropic. As may be seen in Fig. 1, our calculated magnetization curves also fail to cross at a single point. Furthermore, the order of the calculated crossings as a function of field is the same as observed in $YBa_2Cu_3O_{7-\delta}$ [10].

The second derivative of the magnetization can also be calculated using the Maxwell relation

$$\left(\frac{\partial^2 M}{\partial T^2}\right)_H = \left(\frac{\partial (C_H/T)}{\partial H}\right)_T, \tag{4}$$

where $C_H \equiv -T(\partial^2 \mathcal{G}/\partial T^2)_H$ is the specific heat of the sample at constant H [14]. Since Eq. (4) equates the second derivative of one macroscopic quantity to the first derivative of another, it provides a potentially more precise way of determining $(\partial^2 M/\partial T^2)_H$ than a direct calculation of $M(T)$. We have done an MC calculation of $C_H(H,T)$, using the fluctuation-dissipation theorem [15]. Our results are presented in Fig. 1 (inset). Clearly, $d(C_H/T)/dH < 0$ in the vortex liquid phase, which implies, in agreement with experiment [11], that $M(T)$ has negative curvature *throughout* the liquid phase, not just in the vicinity of the mean-field critical temperature $T_{c2}(H)$. The straight lines in Fig. 1 are constructed using slopes determined from independent calculations of the magnetization. To an excellent approximation, they are tangent to the specific heat curves, as expected from Eq. (4), thus confirming the self-consistency of our approach. Experimental specific

heat data [16] confirm that $d(C_H/T)/dH < 0$ in the vortex liquid phase. In the solid phase, our work predicts that $d(C_H/T)/dH > 0$. This is in agreement with recent, high-accuracy specific heat measurements by Schilling and Jeandupeux [17] on large twinned $YBa_2Cu_3O_{7-\delta}$ crystals.

Figure 2 shows the in-plane structure factor $S(\mathbf{q}_\perp, 0)$ defined as the thermal average

$$S(\mathbf{q}_\perp, 0) = \left\langle \int d^3\mathbf{r}\, d^3\mathbf{r}' |\psi(\mathbf{r})|^2 |\psi(\mathbf{r}')|^2 e^{i\mathbf{q}_\perp \cdot (\mathbf{r}-\mathbf{r}')} \right\rangle, \quad (5)$$

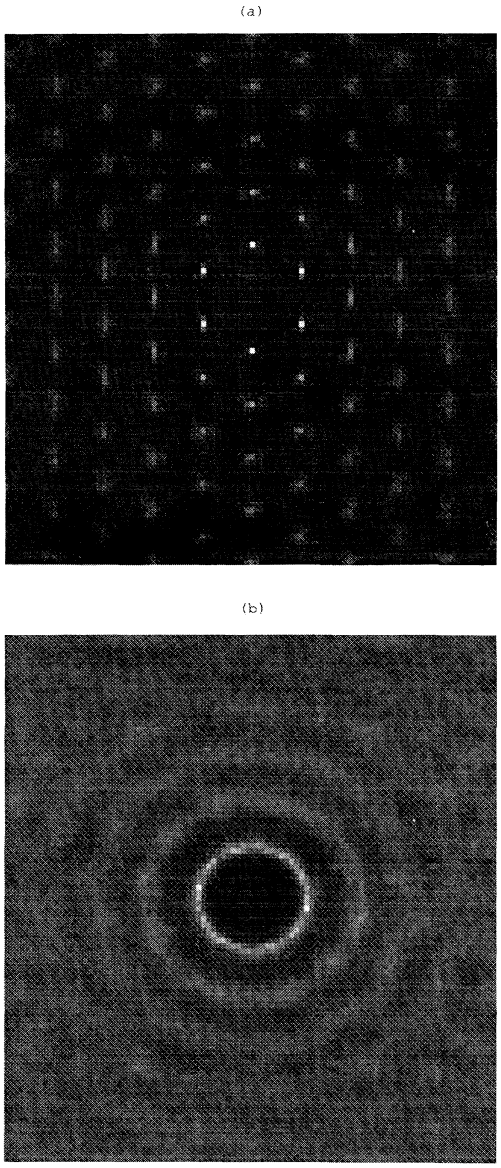

FIG. 2. (a) In-plane structure factor $S(\mathbf{q}_\perp, 0)$, divided by the "atomic" structure factor $\exp(-q_\perp^2/4)$, taken in the solid phase at $T = 82.8$ K and $H = 50$ kOe, and averaged over 100 configurations. The central maximum at $\mathbf{q}_\perp = 0$ has been removed for clarity. (b) Same as (a), but in the liquid phase at $T = 83.0$ K.

for a field $H = 50$ kOe at two temperatures $T = 82.8$ and 83.0 K, corresponding to the vortex solid and vortex liquid phases. This dramatic change occurs at the temperature of the magnetization discontinuity, thus confirming that this discontinuity signals a melting transition. The regular periodic structure of the maxima in Fig. 2(a) corresponds to an ordered crystalline phase, while the concentric rings of Fig. 2(b) characterize an isotropic fluid. In both cases, the deviations from perfect isotropy can be attributed to the finite size of the sample, as well as to its rectangular shape.

Finally, we address the issue of the order of the melting transition. As indicated by Fig. 2, upon melting, the vortex ensemble undergoes a *discontinuous* symmetry change. By the well-known argument of Landau [18], the vortex melting transition has to be first order, with a finite jump in entropy per unit volume ΔS. A critical point (defined by $\Delta S = 0$) cannot exist, and the liquid-solid phase boundary must terminate by intersecting either the coordinate axes or other phase boundaries.

To calculate ΔS, we use a variant of the histogram method of Lee and Kosterlitz [19]. In principle, one should resolve the energy distribution $P(G)$ into two Gaussian peaks at T_m, then confirm that the dip between the peaks scales like a surface energy with increasing sample size [20]. In the present case, this would be a formidable computational effort, because ΔS is small and the two peaks are not resolved at any accessible system sizes. Instead, we perform a long MC run ($\sim 10^6$ passes through the entire lattice) near T_m, starting from the system ground state. During the simulation, the system flips ~ 2–4 times between the two states in equilibrium. In our standard diffusive sampling algorithm, we can identify continuous (in MC "time") sequences of representatives belonging to the same homogeneous phase. The two phases can be clearly distinguished by their structure factors and mean internal energy.

In Fig. 3 we plot the probability distribution of internal energy, $P(G)$, for these two phases in equilibrium at $T_m \sim 83$ K and $H = 50$ kOe, at three system sizes. The low-energy peak always corresponds to the ordered vortex solid phase. Since the entropy change ΔS_ϕ *decreases* with system size, the value $\Delta S_\phi \sim 0.034 k_B$ should be considered an *upper bound* to ΔS_ϕ in the thermodynamic limit. $\Delta S_\phi (H = 20$ kOe) has a similar size dependence and is $\sim 30\%$ smaller than $\Delta S_\phi (H = 50$ kOe).

From our calculated ΔS at melting and the computed slope $(dH/dT)_m$ of the melting curve from Fig. 1, we can estimate the magnetization jump ΔM at melting via the Clausius-Clapeyron relation $\Delta S/\Delta M = -(dH/dT)_m$. Inserting the calculated values of this slope and of ΔS_ϕ, we obtain $\Delta M \sim 0.0014$ emu cm^{-3} at $H = 50$ kOe, and $\Delta M \sim 0.0005$ emu cm^{-3} at $H = 20$ kOe. These values are consistent with the directly calculated ΔM seen in Fig. 1. In experiment, no finite magnetization jump has yet been observed [11,21], although transport measurements on untwinned $YBa_2Cu_3O_{7-\delta}$ crystals are widely

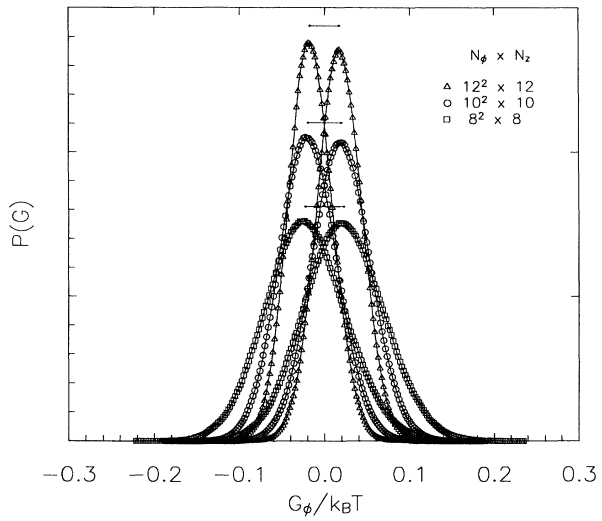

FIG. 3. Probability distribution $P(G)$ of internal energy at the finite-size melting point $T_m \sim 83$ K, $H = 50$ kOe, and three different system sizes. For each system size, the two separate peaks represent the distributions of energy within the solid and the liquid *at the same T and H*. Because of the weak dependence of T_m on system size, we have used for the zero of G_ϕ a size-dependent energy. Horizontal bars denote the calculated latent heats per flux line per layer.

interpreted as evidence for a first-order melting transition [9,22]. The null result of Farrell *et al.* [11] for ΔM puts an upper bound $\Delta S_\phi < 0.003 k_B$ at $H = 20$ kOe, a value almost 10 times smaller than predicted in the present work. However, as suggested by these authors themselves, the presence of defects may have suppressed the measured ΔM to some extent. This discrepancy remains to be settled by an experiment that attains perfect reversibility in both temperature and field.

To summarize, we have presented the first non-mean-field calculation of magnetization in $YBa_2Cu_3O_{7-\delta}$, using a constant-**H** Monte Carlo technique in conjunction with a lowest Landau level approximation. Our results yield a magnetization in very good agreement with experiment in both the flux liquid and flux lattice states, as well as a melting curve very close to experiment. Our results provide perhaps the most detailed evidence to date that a Ginzburg-Landau free energy functional, based on a complex scalar order parameter, adequately describes the thermodynamic properties of $YBa_2Cu_3O_{7-\delta}$ near the flux-lattice melting curve.

We are grateful for valuable conversations with Professor D. E. Farrell, Professor T. R. Lemberger, and Professor W. F. Saam. This work was supported by NSF through Grant No. DMR94-02131, and the Midwest Superconductivity Consortium through DOE Grant No. DE-FG02-90ER45427. The calculations were performed on the local network of DEC Alpha stations.

[1] G. Blatter *et al.*, Rev. Mod. Phys. **66**, 1125 (1994).
[2] D. E. Farrell, in *Physical Properties of High Temperature Superconductors IV,* edited by D. M. Ginsberg (World Scientific, Singapore, 1994).
[3] See, for example, M. Tinkham, *Introduction to Superconductivity* (McGraw-Hill, New York, 1985).
[4] E. H. Brandt, Phys. Rev. Lett. **66**, 3213 (1991).
[5] R. Šášik and D. Stroud, Phys. Rev. B **48**, 9938 (1993).
[6] J. Lee and K. J. Strandburg, Phys. Rev. B **46**, 11 190 (1992).
[7] U. Welp *et al.*, Phys. Rev. Lett. **62**, 1908 (1989).
[8] D. E. Farrell, J. P. Rice, and D. M. Ginsberg, Phys. Rev. Lett. **67**, 1165 (1991).
[9] H. Safar *et al.*, Phys. Rev. Lett. **69**, 824 (1992).
[10] U. Welp *et al.*, Phys. Rev. Lett. **67**, 3180 (1991).
[11] D. E. Farrell *et al.*, Phys. Rev. B **51**, 9148 (1995).
[12] L. N. Bulaevskii, M. Ledvij, and V. G. Kogan, Phys. Rev. Lett. **68**, 3773 (1992).
[13] Z. Tešanović *et al.*, Phys. Rev. Lett. **69**, 3563 (1992).
[14] In actuality C_H is just the superconducting part of the specific heat of a crystal.
[15] Care must be taken here, for $G[\psi, \mathbf{A}]$ is explicitly temperature dependent.
[16] S. E. Inderhees *et al.*, Phys. Rev. Lett. **66**, 232 (1991).
[17] A. Schilling and O. Jeandupeux (unpublished).
[18] L. D. Landau and E. M. Lifshitz, *Statistical Physics* (Pergamon Press, New York, 1989), 3rd ed., Part 1, p. 258.
[19] J. Lee and J. M. Kosterlitz, Phys. Rev. Lett. **65**, 137 (1990).
[20] R. Hetzel, A. Sudbø, and D. A. Huse, Phys. Rev. Lett. **69**, 518 (1992); Y. Kato and N. Nagaosa, Phys. Rev. B **48**, 7383 (1993); J. Hu and A. H. MacDonald, Phys. Rev. Lett. **71**, 432 (1993); J. Hu, Ph.D. thesis, Indiana University, 1994.
[21] A reversible magnetization jump in $Bi_2Sr_2CaCu_2O_{8+\delta}$ has been recently reported by E. Zeldov *et al.*, Nature (London) **375**, 373 (1995).
[22] H. Safar *et al.*, Phys. Rev. Lett. **70**, 3800 (1993); W. K. Kwok *et al.*, Phys. Rev. Lett. **69**, 3370 (1992); W. K. Kwok *et al.*, Phys. Rev. Lett. **72**, 1092 (1994).

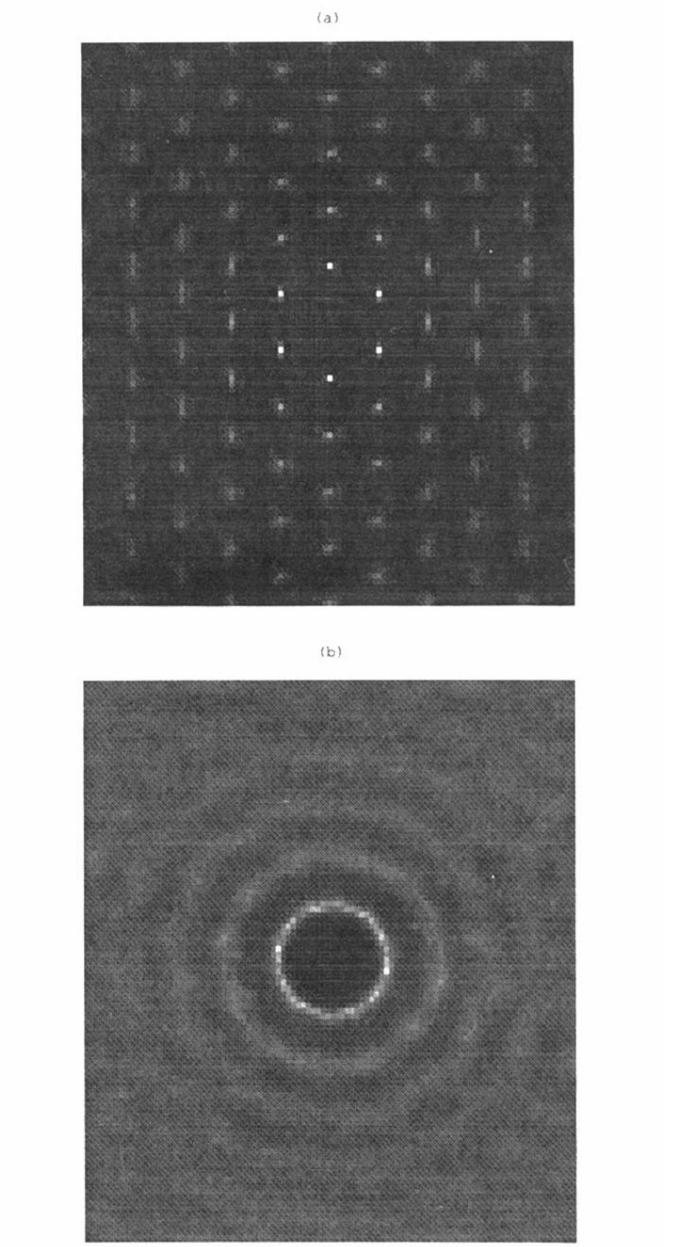

FIG. 2. (a) In-plane structure factor $S(\mathbf{q}_\perp, 0)$, divided by the "atomic" structure factor $\exp(-q_\perp^2/4)$, taken in the solid phase at $T = 82.8$ K and $H = 50$ kOe, and averaged over 100 configurations. The central maximum at $\mathbf{q}_\perp = 0$ has been removed for clarity. (b) Same as (a), but in the liquid phase at $T = 83.0$ K.